



Dynamo Action in a Shell Model for MHD Turbulence

2nd UN/NASA Workshop on IHY and Basic Space Science

Ganapati Sahoo ^a, Dhrubaditya Mitra ^b, and Rahul Pandit ^c

^aDepartment of Physics, Indian Institute of Science, INDIA, email: ganapati@physics.iisc.ernet.in

^bObservatoire de la Côte d'Azur, Nice, FRANCE, email: Dhrubaditya.MITRA@obs-nice.fr

^cDepartment of Physics, Indian Institute of Science, Bangalore, INDIA, email: rahul@physics.iisc.ernet.in



Introduction

- What is a Dynamo?
 - ❖ The amplification of weak magnetic fields in a turbulent conducting fluid because of the stretching of field lines by randomly moving fluid elements.
 - ❖ Eddies of size l and velocity $v(l) \sim l^{1/3}$ have a rate of shearing $\frac{v(l)}{l} \sim l^{-2/3}$.
 - ❖ Kinematic dynamo: initial amplification; the magnetic field is too small to affect the velocity field.



Introduction

- Dimensionless Parameters

- ◆ kinetic Reynolds number $Re = \frac{VL}{\nu}$;

- ◆ magnetic Reynolds number $R_m = \frac{VL}{\eta}$;

- ◆ magnetic Prandtl number $Pr_m = \frac{R_m}{Re} = \frac{\nu}{\eta}$.

L, V, ν, η : characteristic length scale, characteristic velocity, kinematic viscosity, and magnetic diffusivity, respectively.

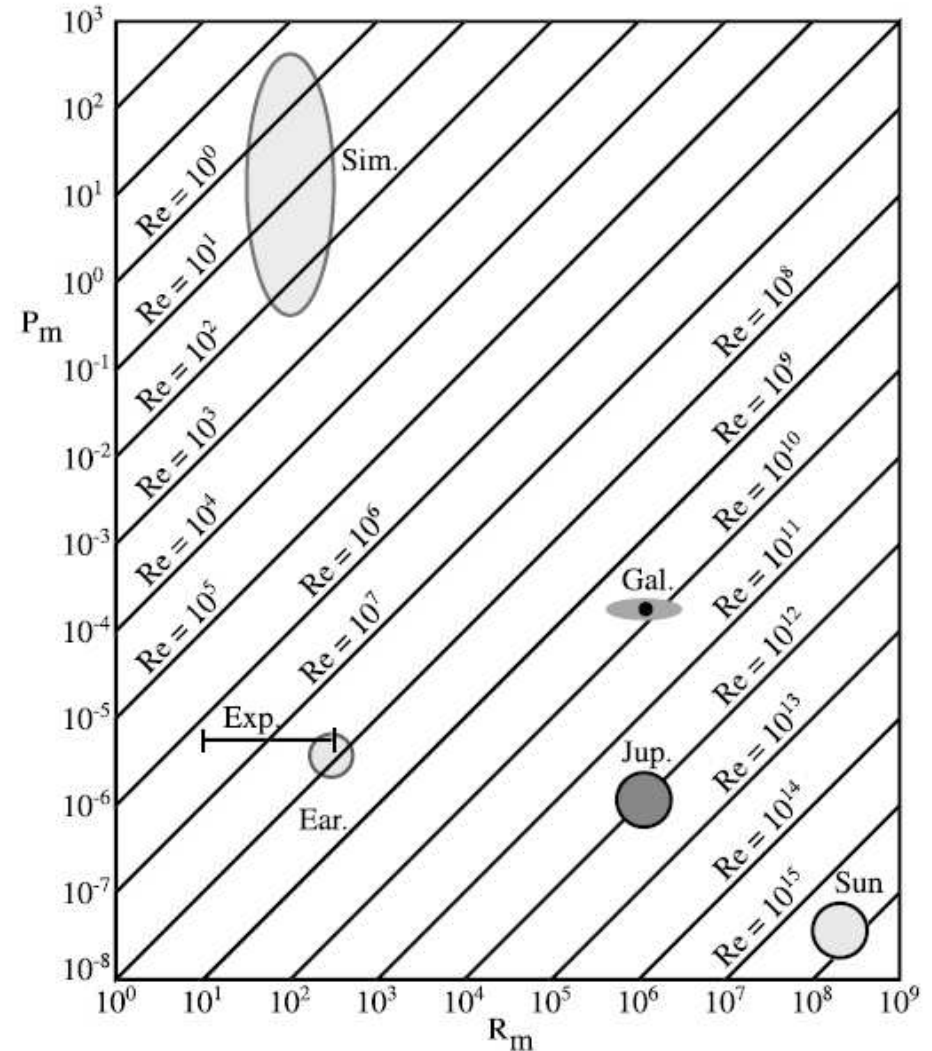


Introduction

- Why do we study dynamo action?
 - ❖ Magnetic fields in geodynamos[1], celestial bodies[2], and the interstellar medium[3].
 - ❖ Experiments on liquid-metal dynamos[3].
- Challenges:
 - ❖ To elucidate the dependence of the critical R_m for dynamo action on Pr_m .
 - ❖ Wide range of Pr_m : ($\sim 10^{-5}$ to $\sim 10^{14}$).
 - ❖ Dynamo action is obtained only for values of R_m that are sufficiently large to overcome *Joule dissipation*.

Dynamo Regimes

Figure 1: R_m and Pr_m for the Earth (Ear), numerical simulations (Sim), Jupiter (Jup), the Sun, estimates for galaxies (Gal) and laboratory experiments (Exp) [after Fauve and Lathrop[3]].



Dynamo Regimes

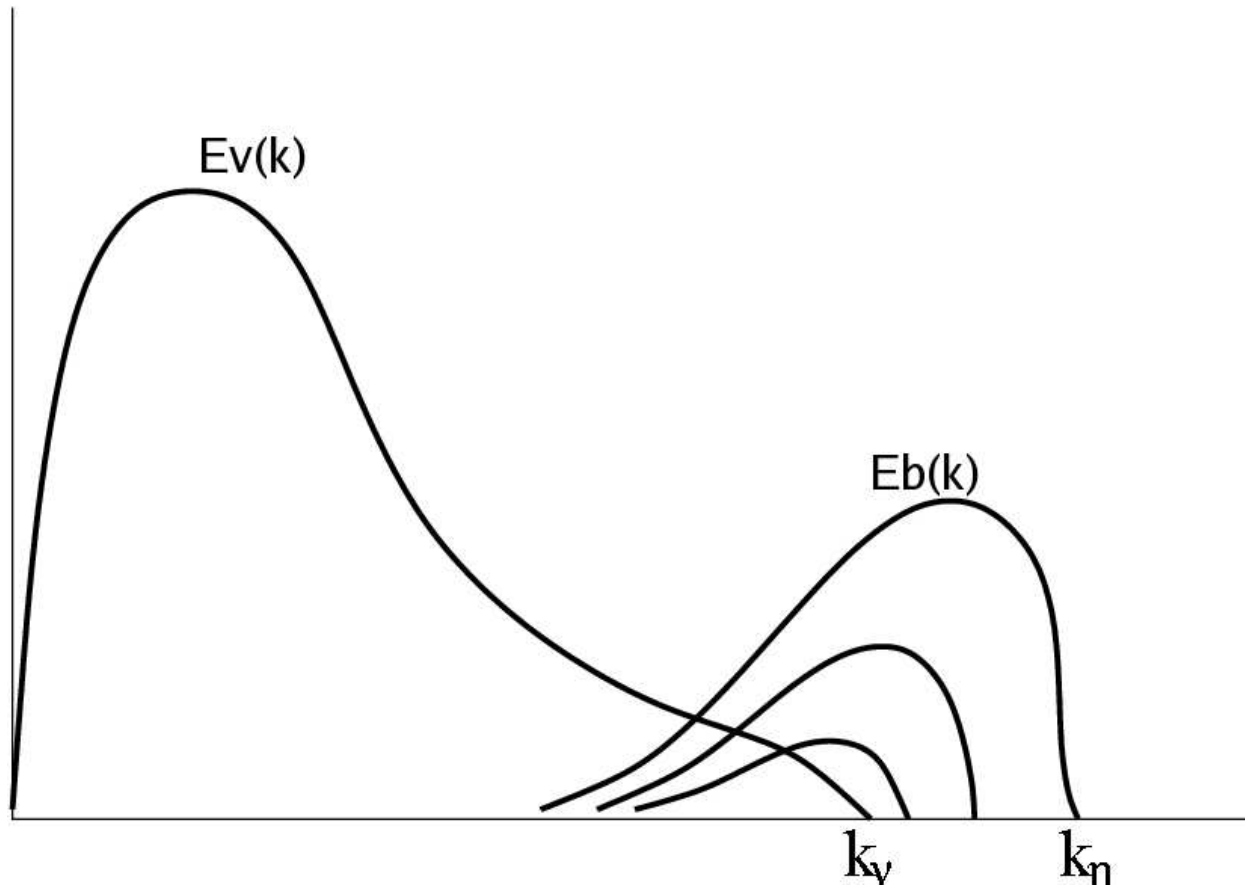


Figure 2: Sketch of the initial growth of the magnetic field in a small-scale dynamo.



Dynamo Regimes

- Large-Prandtl-number regime ($Pr_m \gg 1$):
 - ❖ Dynamo action in astronomical settings.
 - ❖ The resistive scale is smaller than the viscous-dissipation scale. Hence the magnetic field grows predominantly in the dissipation range, i.e., we have a small-scale dynamo[4].
- Small-Prandtl-number regime ($Pr_m \ll 1$):
 - ❖ Dynamo action in constrained flows of liquid sodium; $Pr_m \sim 10^{-5}$.
 - ❖ Growth of the magnetic field in the inertial range of the fluid.



Magnetohydrodynamics

Hydrodynamics of a conducting fluid:

$$\frac{\partial \vec{u}}{\partial t} + (\vec{u} \cdot \vec{\nabla}) \vec{u} = \nu \Delta \vec{u} - \vec{\nabla} \bar{p} + \frac{1}{4\pi} (\vec{b} \cdot \vec{\nabla}) \vec{b} + \vec{f}; \quad (1)$$

$$\frac{\partial \vec{b}}{\partial t} = \vec{\nabla} \times (\vec{u} \times \vec{b}) + \eta \Delta \vec{b}. \quad (2)$$

\vec{u} , \vec{b} , p , ν , η , \vec{f} : velocity field, magnetic field, pressure, kinematic viscosity, magnetic diffusivity, and external force, respectively;

$$\bar{p} \equiv p + \frac{b^2}{8\pi}. \quad (3)$$

Incompressibility and divergenceless conditions:

$$\vec{\nabla} \cdot \vec{u}(\vec{x}, t) = 0; \quad \vec{\nabla} \cdot \vec{b}(\vec{x}, t) = 0. \quad (4)$$



Pseudospectral Method

- Initial velocities and magnetic fields: in Fourier space.
- Nonlocal terms like $\vec{\nabla} \times (\vec{u} \times \vec{b})$, $\vec{\nabla} \times \vec{u}$, etc., are calculated in Fourier space.
- Terms like $\vec{u} \times \vec{b}$ are calculated in real space.
- We switch between real and Fourier space by an FFT algorithm.
- For the first time step we use a Runge-Kutta scheme.
- An Adams-Bashforth second-order scheme is used for temporal evolution after that.



A Shell Model for MHD

A. Basu, *et al*, [5] and Sokoloff, *et al*, [6] - 1998

$$\begin{aligned} \frac{du_n}{dt} + \nu k_n^2 u_n &= i[A_n(u_{n+1}u_{n+2} - b_{n+1}b_{n+2}) \\ &+ B_n(u_{n-1}u_{n+1} - b_{n-1}b_{n+1}) \\ &+ C_n(u_{n-2}u_{n-1} - b_{n-2}b_{n-1})] + f_n. \end{aligned} \quad (5)$$

$$\begin{aligned} \frac{db_n}{dt} + \eta k_n^2 b_n &= i[D_n(u_{n+1}b_{n+2} - b_{n+1}u_{n+2}) \\ &+ E_n(u_{n-1}b_{n+1} - b_{n-1}u_{n+1}) \\ &+ F_n(u_{n-2}b_{n-1} - b_{n-2}u_{n-1})]; \end{aligned} \quad (6)$$

the velocity u_n and the magnetic field b_n in shell n are complex, scalar

variables.



A Shell Model for MHD

The shells are logarithmically spaced in Fourier space, i.e., $k_n = k_0 2^n$ and, to ensure the conservation of energy and helicity in the *unforced and inviscid* limit, we choose

$$\begin{aligned} A_n &= k_n; & B_n &= -k_{n-1}/2; & C_n &= -k_{n-2}/2; \\ D_n &= k_n/6; & E_n &= k_{n-1}/3; & F_n &= -2k_{n-2}/3; \\ f_n &= (1 + i) \times 5 \times 10^{-3} \times \delta_{n,1}. \end{aligned} \tag{7}$$

ν and η are the kinematic viscosity and the magnetic diffusivity, respectively.



Numerical Scheme

For an equation of the form

$$\frac{dq}{dt} = -\alpha q + f(t) \quad (8)$$

we use the following *fifth-order Adams-Bashforth* scheme:

$$\begin{aligned} q(t + \delta t) &= e^{-2\alpha\delta t} q(t - \delta t) + \frac{1 - e^{-2\alpha\delta t}}{24\alpha} \\ &\times [55f(t) - 59f(t - \delta t) \\ &+ 37f(t - 2\delta t) - 9f(t - 3\delta t)]. \end{aligned} \quad (9)$$

This scheme works well if the total number of shells $N \lesssim 35$ and $Re \lesssim 10^9$.



Numerical Scheme

- In all our calculations $\delta t = 10^{-4}$, $N = 30$.
- Characteristic time scales:
 - ◆ Diffusion time: $\tau_\eta = \frac{L^2}{\eta}$.
 - ◆ Large-eddy-turnover time: $\tau_L = \frac{L}{v_{rms}}$.



Goals

- How does the magnetic energy grow at different scales for low values of Pr_m ?
- Is there an absolute dynamo boundary in the R_m and Pr_m plane?
- Does the time required for dynamo action depend on R_m and Pr_m ?
- Direct Numerical Simulations (DNS) have been carried out typically in the range $Pr_m \sim 1$; it is important to extend such studies to values of Pr_m that lie in the experimental ranges mentioned above.

We have carried out an extensive numerical study, with our high-order numerical scheme, to determine the dynamo boundary in our shell model over a wide range of R_m and Pr_m (many orders of magnitude greater than the range possible in a DNS of the MHD equations[7]).

Energy Spectra

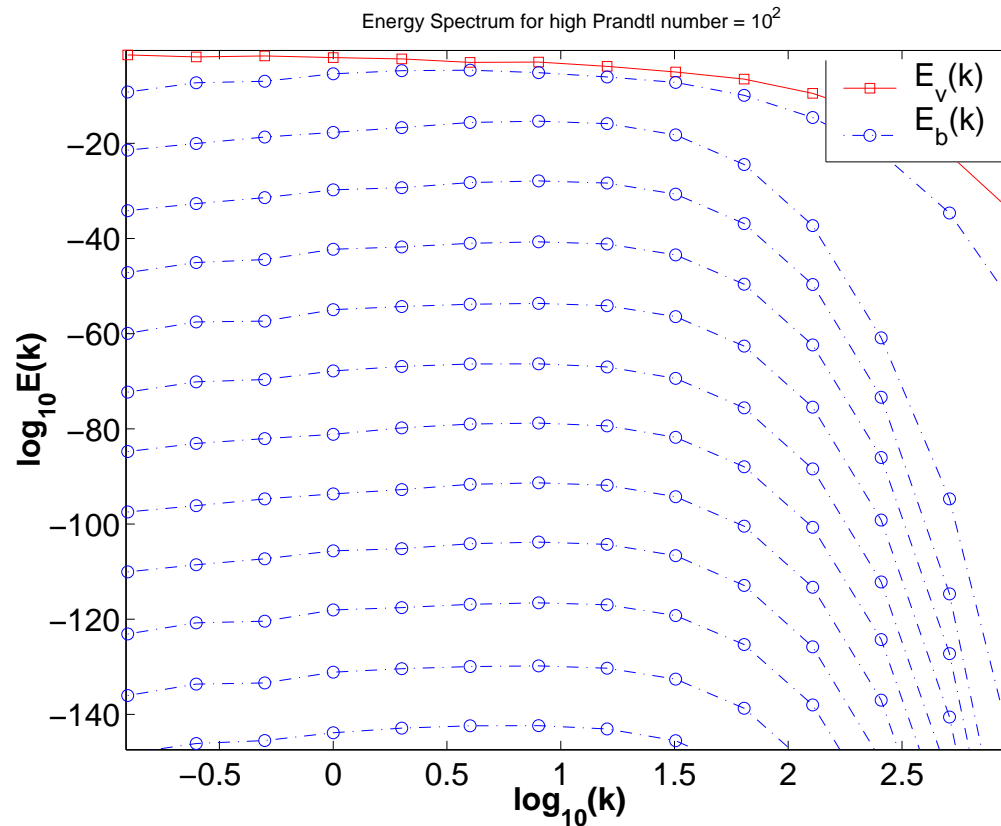


Figure 3: Evolution of energy spectra in the kinematic regime and at high Prandtl numbers, e.g., $Pr_m = 10^2$, the magnetic energy grows predominantly in the dissipation range; after the saturation of the dynamo, Kolmogorov-type $-5/3$ spectra are obtained.

Energy Spectra

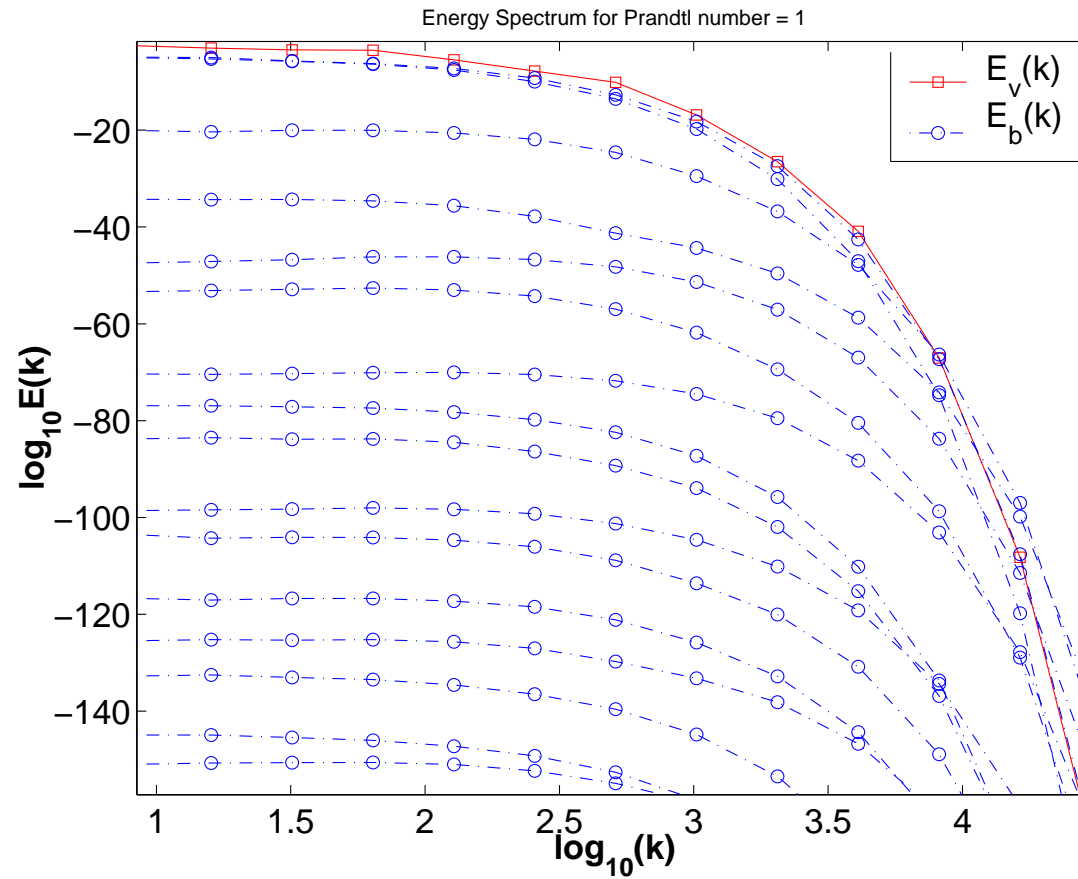


Figure 4: Evolution of energy spectra in the kinematic regime for $Pr_m = 1$

Energy Spectra

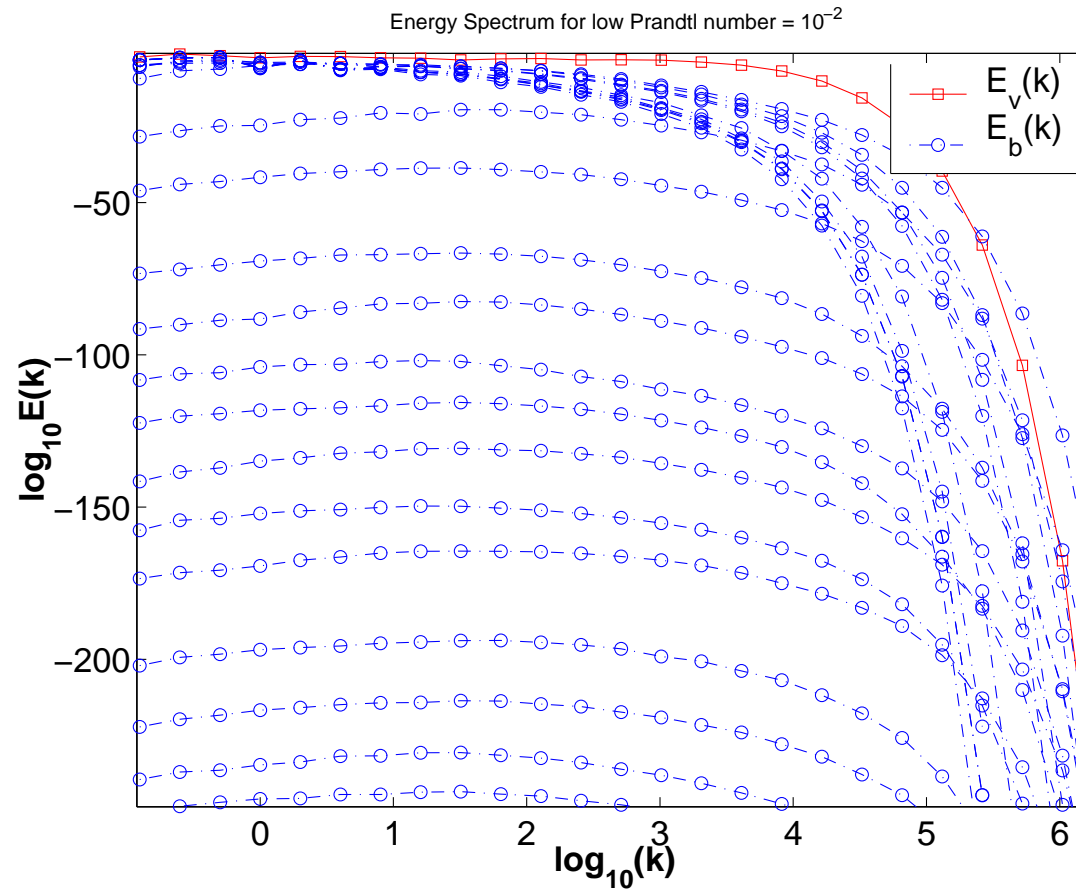


Figure 5: Evolution of energy spectra in the kinematic regime for low Prandtl numbers like $Pr_m = 10^{-2}$; the magnetic energy grows in the inertial range as well as in the dissipation range.

Temporal Evolution

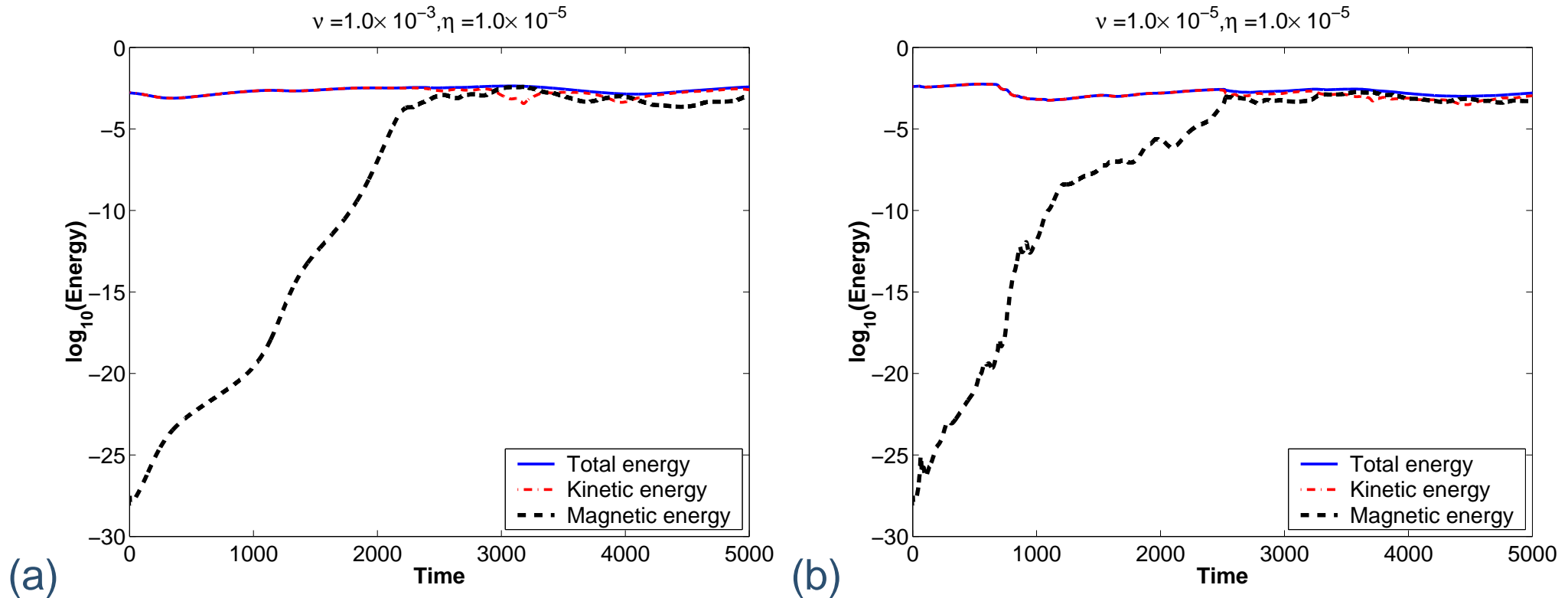


Figure 6: Growth of the magnetic energy for high Prandtl numbers: (a) $Pr_m = 10^2$; (b) $Pr_m = 1$.

Temporal Evolution

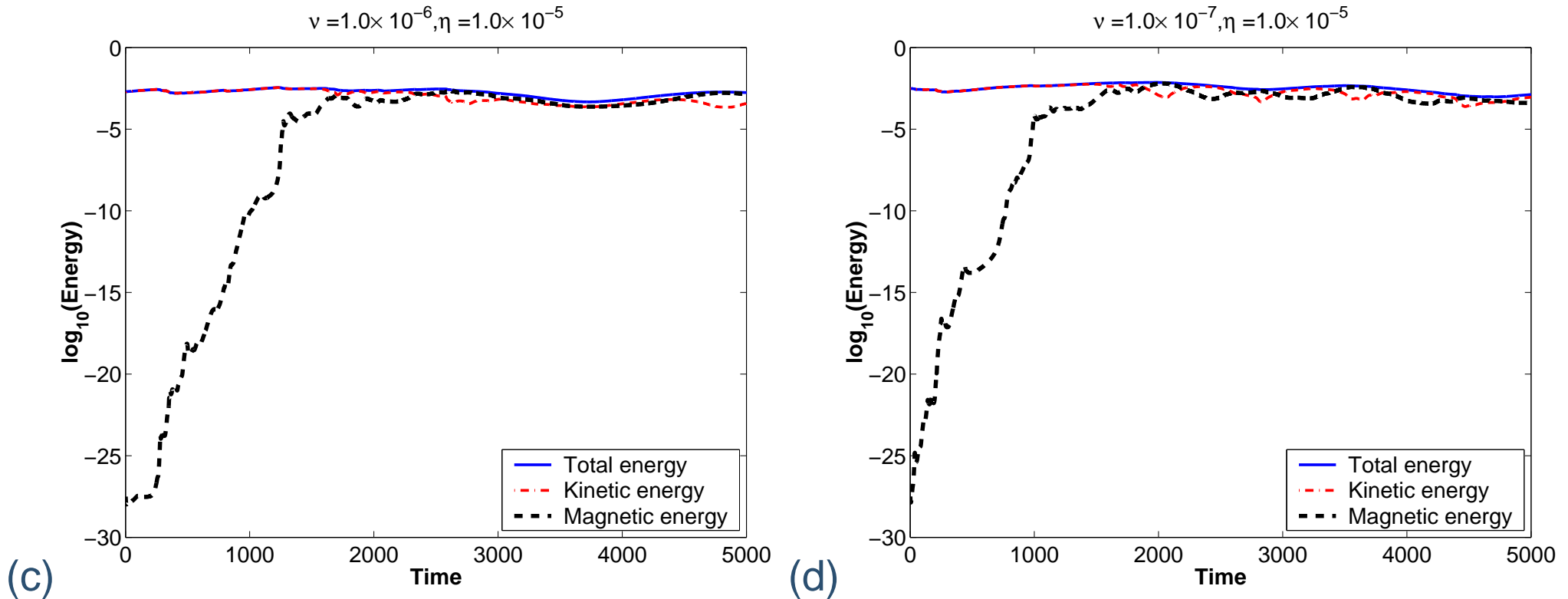


Figure 7: Growth of the magnetic energy for low Prandtl numbers: (c) $Pr_m = 10^{-1}$; (d) $Pr_m = 10^{-2}$.

Temporal Evolution

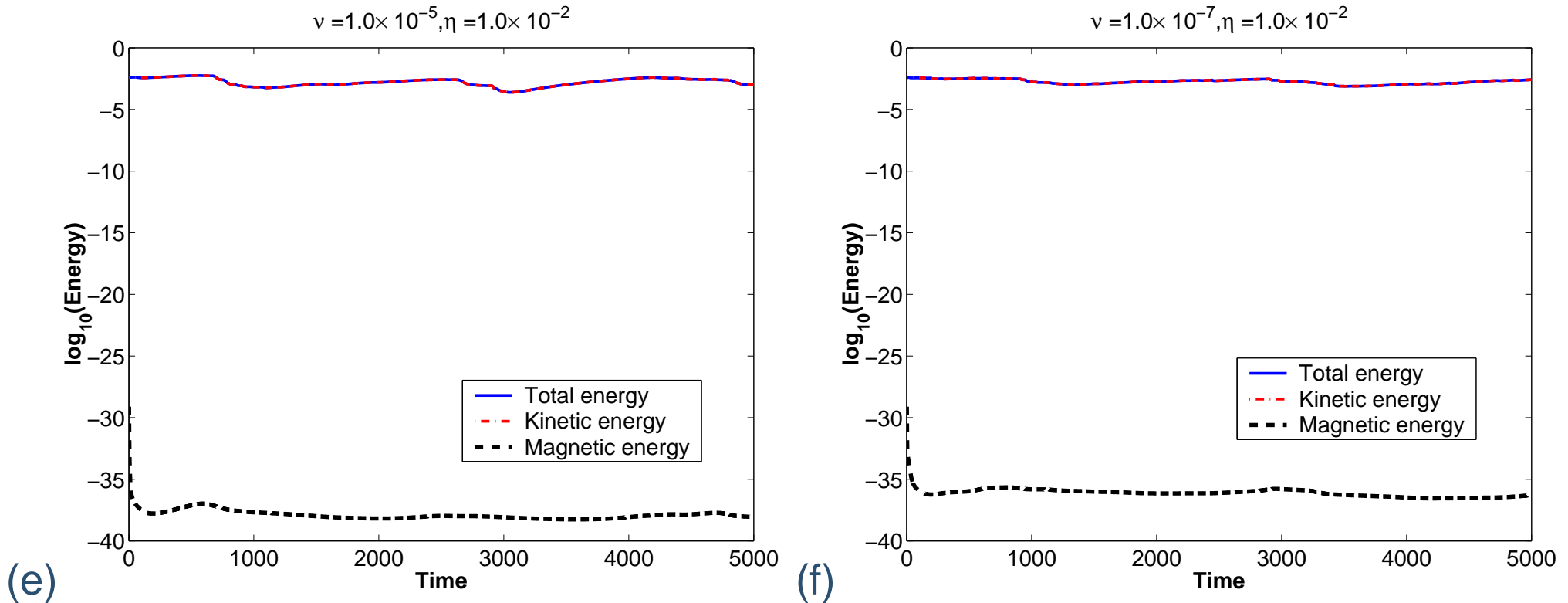


Figure 8: Decay of the magnetic energy for low Prandtl numbers; (e) $Pr_m = 10^{-3}$; (f) $Pr_m \sim 10^{-5}$.

Temporal Evolution

Ponty et al

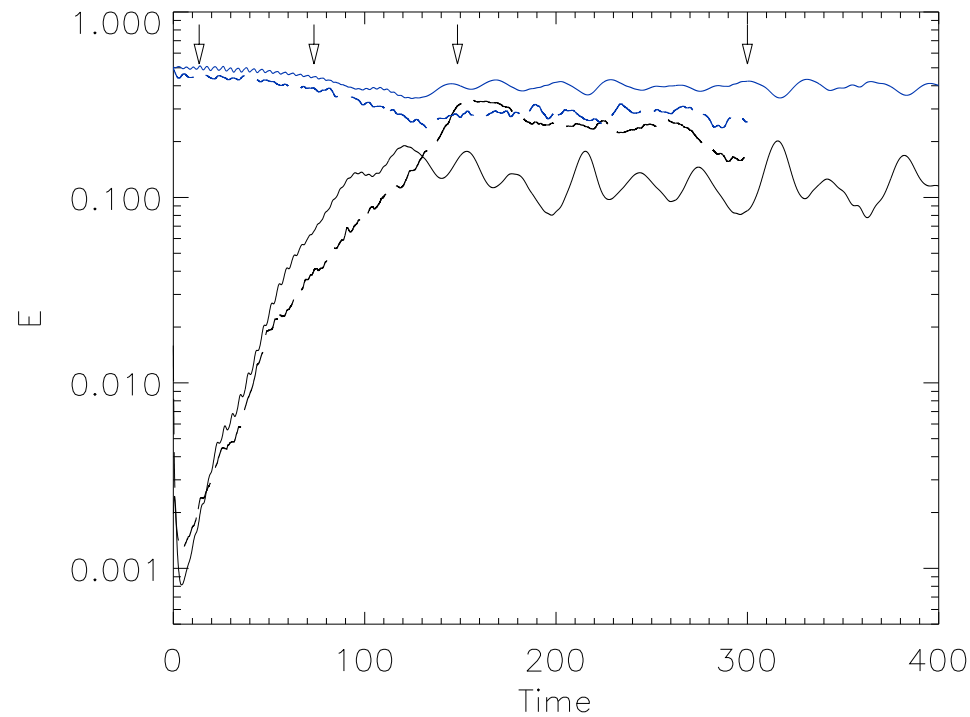


Figure 9: Evolution of kinetic (upper curve) and magnetic energy (lower curve) for $R_e = 40.5$, $R_m = 37.8$ (solid lines) and $R_e = 675$, $R_m = 270$ (dotted lines), both 20% above threshold.



Stability Boundary

- Initial velocity: Statistically stabilised velocities from the GOY shell model.
- Initial seed magnetic field: $b(k) = 10^{-8} \times \sqrt{E_v(k)} \exp(i\theta)$, where θ is a random phase.
- If we use a fixed dynamo threshold, say $E_b = 10^{-6}$, we find that the dynamo boundary depends on the simulation time.
- Some authors suggest[7] that the simulation should be run for a time $\sim \tau_\eta$.
- We find that far shorter runs suffice to obtain the asymptotic dynamo boundary.

Stability Boundary

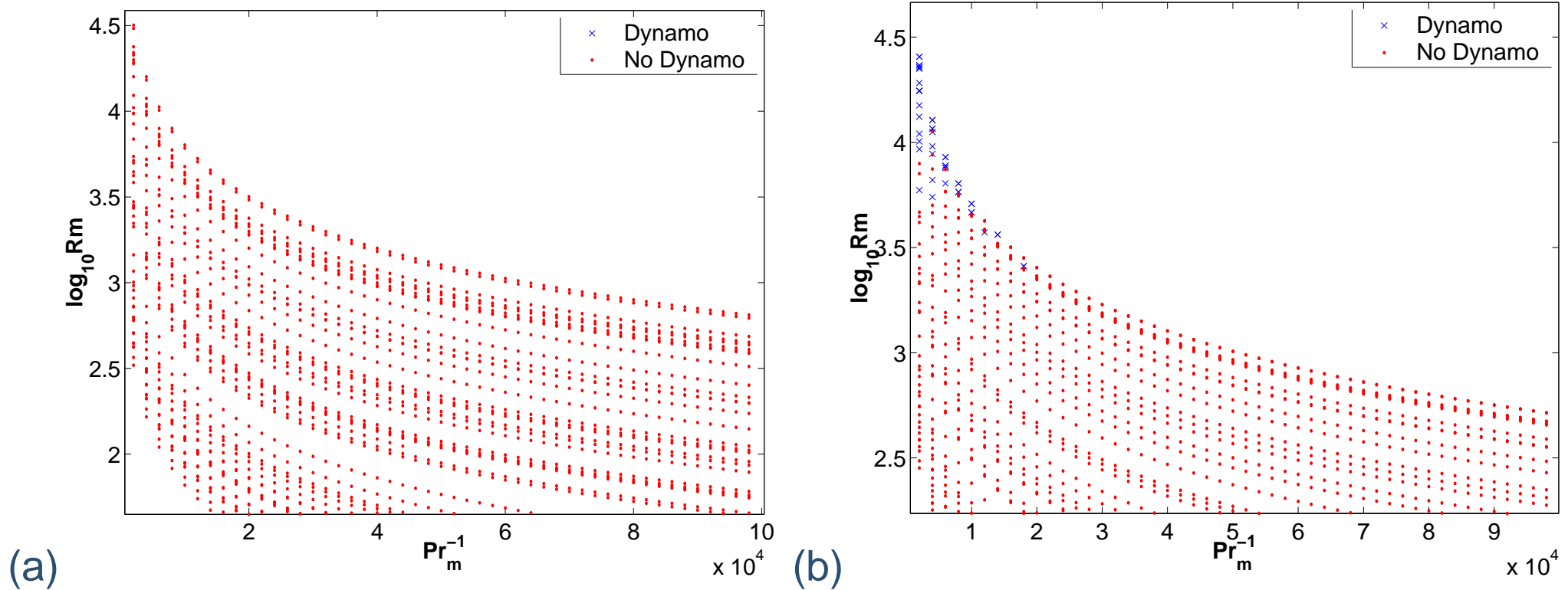


Figure 10: Stability diagram in the $R_m - Pr_m^{-1}$ plane showing the temporal evolution of the dynamo boundary: (a) 5.0×10^7 time steps; (b) 2.0×10^8 time steps.

Stability Boundary

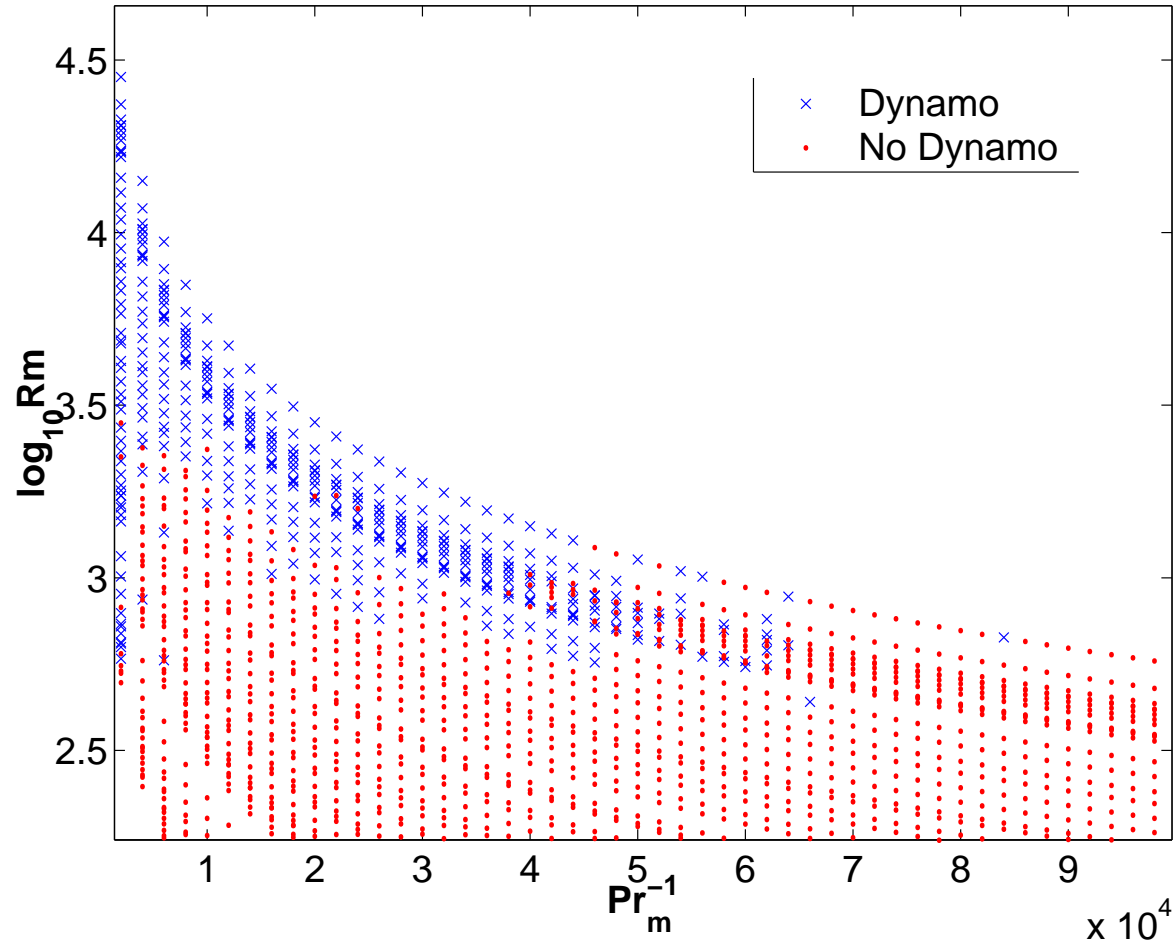


Figure 11: Stability diagram in the $R_m - Pr_m^{-1}$ after 5.0×10^8 time steps.

Stability Boundary

Ponty et al

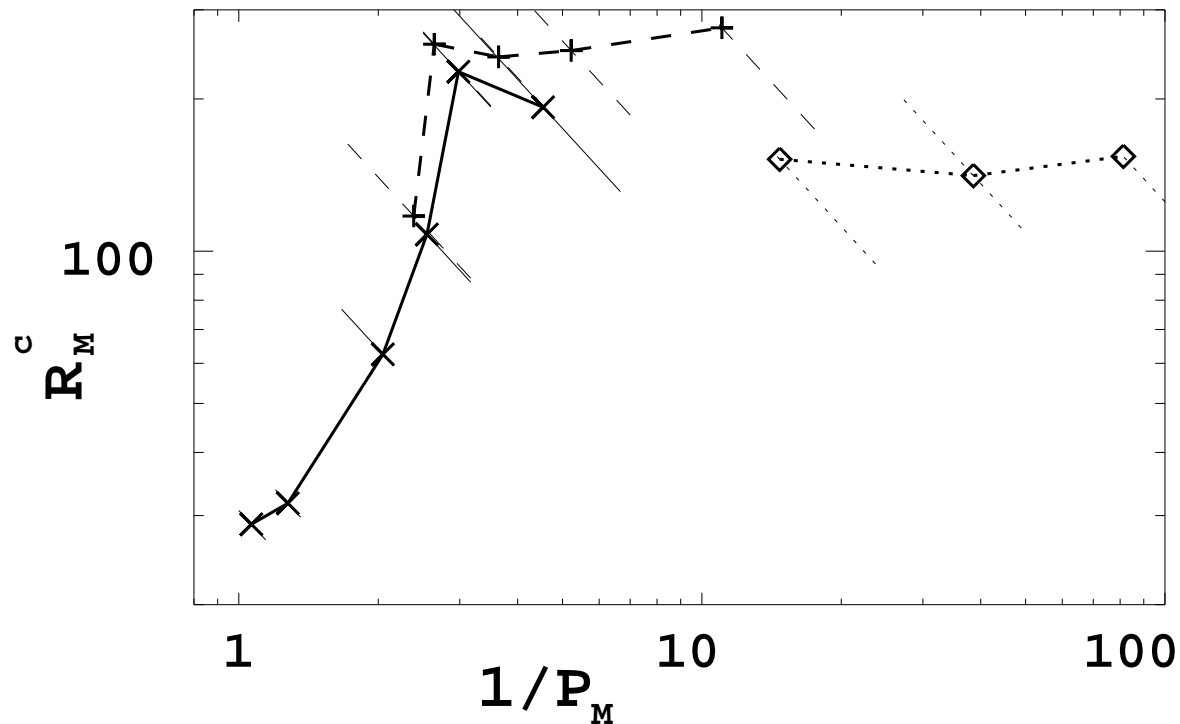


Figure 12: R_M^c for dynamo action versus inverse P_M . Symbols are: \times (DNS), $+$ (LAMHD), and \diamond (LES). Transverse lines indicate error bars in the determination of R_M^c , as the distance between growing and decaying runs at a constant R_V .



Criterion for Dynamo Action

- Once the magnetic field saturates it never decays (barring very small fluctuations); we have checked this for representative points in the stability diagram.
- Initial seed magnetic field (random phases): $E_b^0 \sim 10^{-28}$ [the same for all the parameters (like ν , η , etc.)].
- We say that dynamo action has occurred if $E_b/E_u \gtrsim 0.9$ (initial kinetic energy $E_u^0 \sim 10^{-5}$); the time required for this is τ_C and it is typically $\ll \tau_\eta$.
- We say that no dynamo action occurs if E_b falls below 10^{-35} .
- The boundary obtained in this way does not change with time.



Criterion for Dynamo Action

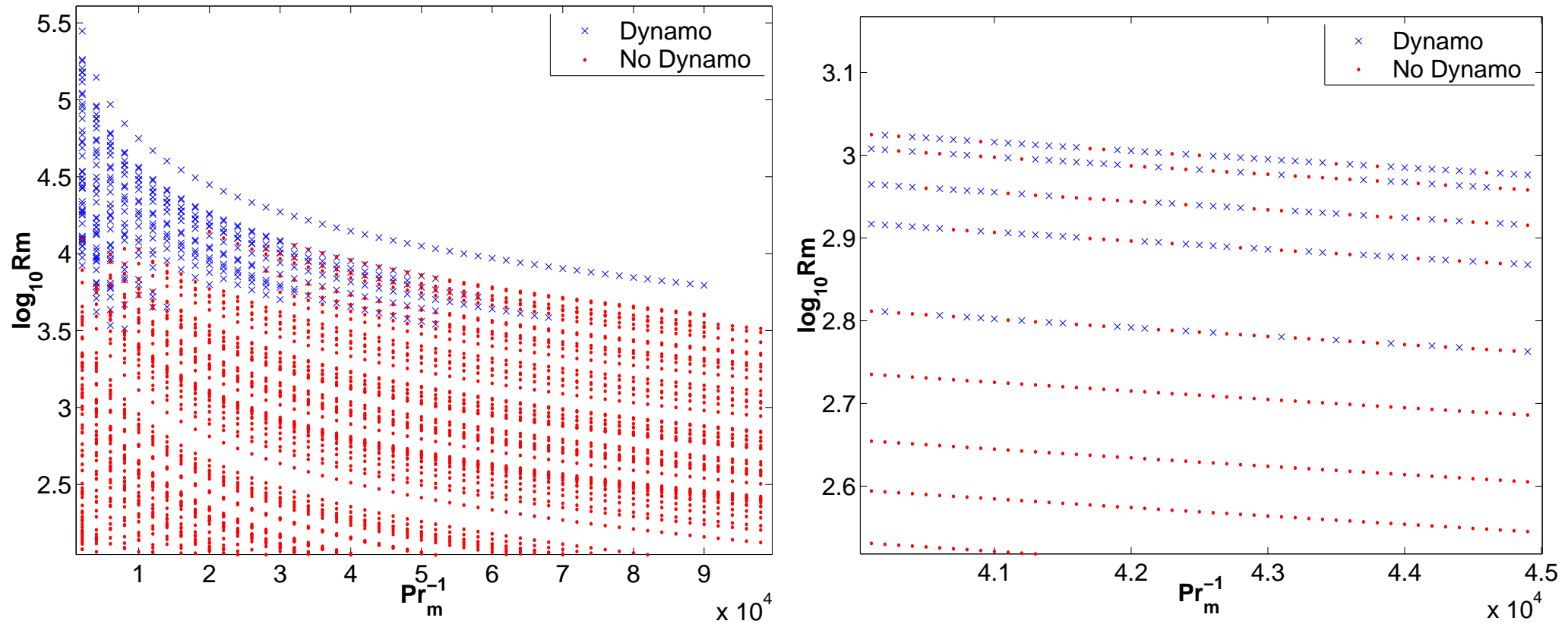


Figure 13: (a) Absolute stability diagram in the $R_m - Pr_m^{-1}$ plane; (b) a magnified view of the boundary that shows its fractal nature.

Results[8]

Order parameter: $\frac{E_b}{E_u}$ in the long-time limit; it jumps at the dynamo boundary.

The time required for dynamo action τ_C seems to diverge as $\tau_C \sim (R_m - R_{mb})^{-\alpha}$, where R_{mb} is the value of R_m at the dynamo boundary (for fixed Pr_m).

The exponent α depends on Pr_m .

$\tau_C = \infty$ in the region in which dynamo action does not occur.

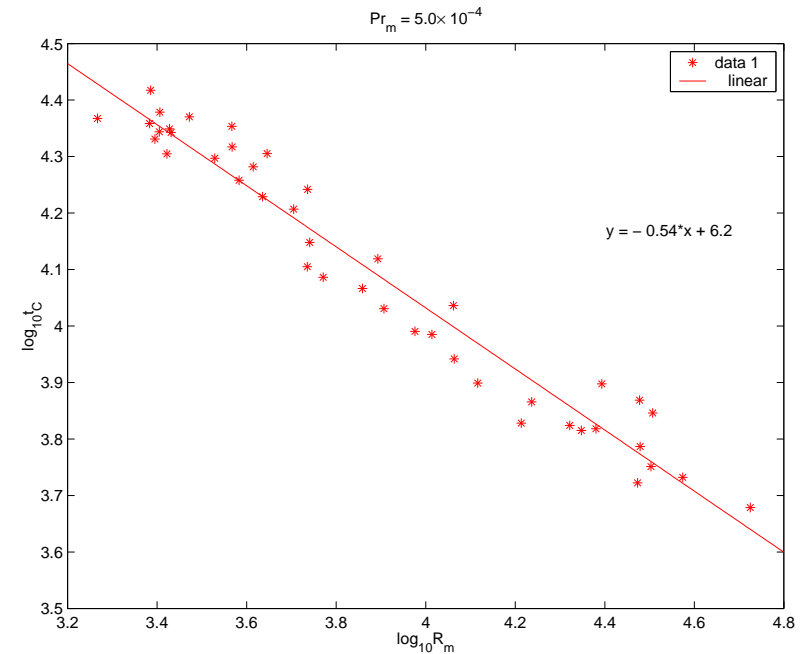


Figure 14: Divergence of τ_C at $Pr_m = 5.0 \times 10^{-4}$

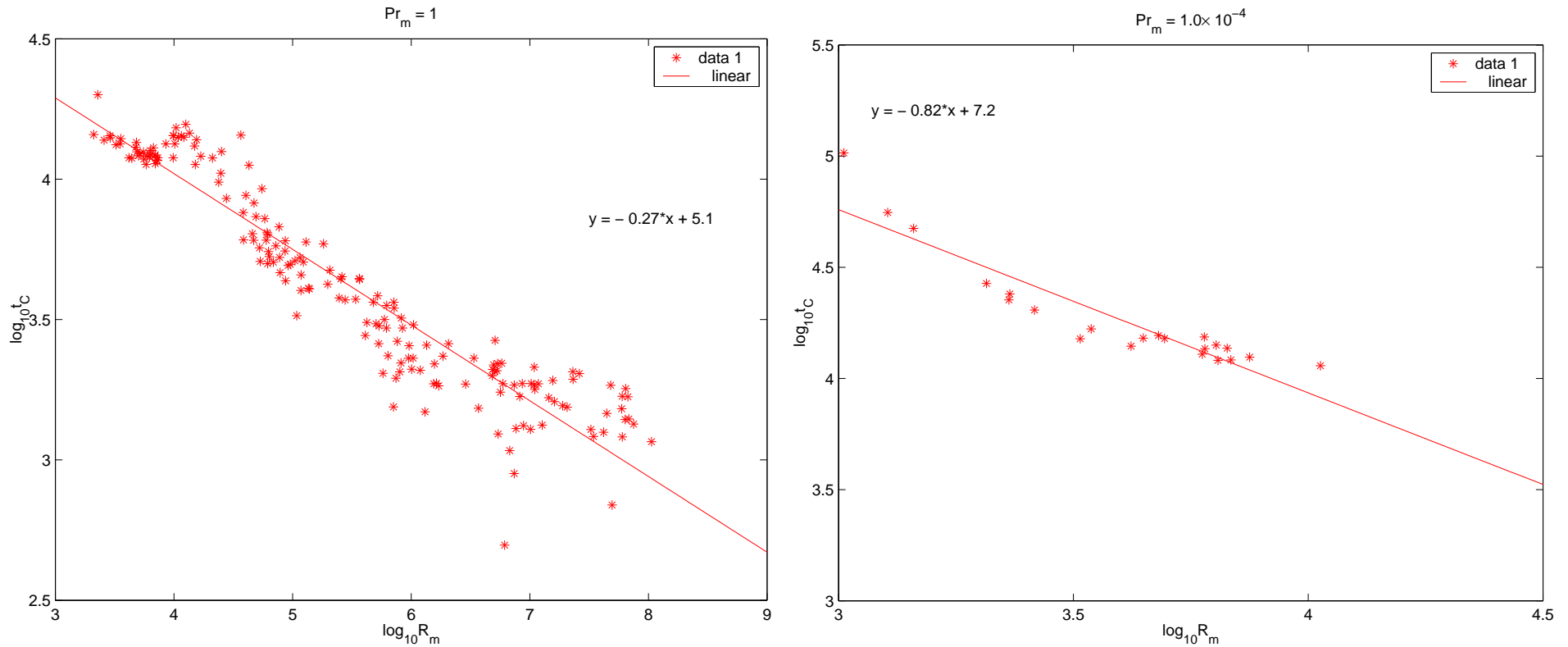


Figure 15: Plots illustrating the divergence of τ_C as we approach the dynamo boundary.



Results[8]

- Our high-precision study of dynamo action in a shell model for MHD turbulence shows that the dynamo boundary in the (R_m, Pr_m^{-1}) plane saturates at large values of Pr_m^{-1} .
- The region of the (R_m, Pr_m^{-1}) that we explore is many orders of magnitude larger than in any earlier study.
- Energy equipartition, i.e., $E_b \sim E_v$, is obtained after the dynamo action has saturated.
- The dynamo boundary appears to be a fractal.



References

● References

- [1] P.H. Roberts and G. A. Glatzmaier, *Rev. Mod. Phys.* **72**, 1081 (2000).
- [2] A.A. Schekochihin, S.C. Cowley, S.F. Taylor, J.L. Maron, and J.C. McWilliams, *Astrophysical Journal* **612**, 276 (2004).
- [3] S. Fauve and D. Lathrop, *The dynamo effect* (2005).
- [4] S. Boldyrev and F. Cattaneo, *Phys. Rev. Lett.* **92**, 144501 (2004).
- [5] A. Basu, A. Sain, S. Dhar, and R. Pandit, *Phys. Rev. Lett.*, **81**, 2687 (1998).
- [6] See also P. Frick and D. Sokoloff, *Phys. Rev. E*, **57**, 4155 (1998); P. Giulani and V. Carbone, *Europhys. Lett.* **43** 527 (1998).
- [7] Y. Ponty, P.D. Mininni, D.C. Montgomery, J.F. Pinton, H. Politano, and A. Pouquet, *Phys. Rev. Lett.* **94**, 164502 (2005); Y. Ponty, H. Politano, and J. F. Pinton, *Phys. Rev. Lett.* **92**, 144503 (2004).
- [8] G. Sahoo, D.Mitra, and R. Pandit, to be published (2006).

● Acknowledgements

- ❖ R. Karan, P. Perlekar, and M. Das.
- ❖ CSIR and DST, India.